

1 **Altered basal lipid metabolism underlies the functional impairment**
2 **of naive CD8⁺ T cells in elderly humans**

3
4 **Brief title:** Metabolic properties of old naive CD8⁺ T cells

5
6 Francesco Nicoli,^{a,b,*} Mariela P. Cabral-Piccin,^{a,1} Laura Papagno,^{a,1} Eleonora Gallerani,^b Victor
7 Folcher,^a Marion Dubois,^a Emmanuel Clave,^c H el ene Vallet,^{a,d} Justin J. Frere,^e Emma Gostick,^f
8 Sian Llewellyn-Lacey,^f David A. Price,^{f,g} Antoine Toubert,^{c,h} Jacques Boddaert,^{a,d} Antonella
9 Caputo,^b Riccardo Gavioli,^b and Victor Appay^{a,i,*}

10
11 ^a Centre d'Immunologie et des Maladies Infectieuses (CIMI-Paris), Sorbonne Universit e,
12 INSERM U1135, 75013 Paris, France

13 ^b Department of Chemical and Pharmaceutical Sciences, University of Ferrara, Ferrara 44121,
14 Italy

15 ^c Institut de Recherche Saint Louis, EMIly, Universit e de Paris, INSERM U1160, 75010 Paris,
16 France

17 ^d Service de G eriatrie, H opital Piti e-Salp etri re, AP-HP, 75013 Paris, France

18 ^e Department of Immunobiology and the Arizona Center on Aging, University of Arizona College
19 of Medicine Tucson, Tucson, AZ 85724, USA

20 ^f Division of Infection and Immunity, Cardiff University School of Medicine, Cardiff CF14 4XN,
21 UK

22 ^g Systems Immunity Research Institute, Cardiff University School of Medicine, Cardiff CF14
23 4XN, UK

24 ^h Laboratoire d'Immunologie et d'Histocompatibilit e, H opital Saint-Louis, AP-HP, 75010 Paris,
25 France

26 ⁱ International Research Center of Medical Sciences, Kumamoto University, Kumamoto 860-
27 0811, Japan

28
29 ¹ These authors contributed equally

30
31 * Correspondence: Francesco Nicoli, nclfnc1@unife.it, Department of Chemical and
32 Pharmaceutical Sciences, University of Ferrara Via Fossato di Mortara 64/B, IV piano 44121
33 Ferrara, Italy.

34 Or Victor Appay, victor.appay@inserm.fr, ImmunoConcEpT, CNRS, Universit e de Bordeaux,
35 146 rue L eo Saignat, 33076 Bordeaux, France

38 **ABSTRACT**

39

40 *Background:* Aging is associated with functional deficits in the naive T cell compartment, which

41 compromise the generation of *de novo* immune responses against previously unencountered

42 antigens. The mechanisms that underlie this phenomenon have nonetheless remained unclear.

43 *Methods:* Biochemical and functional properties of naive CD8⁺ T cells were characterized and

44 compared between middle aged and older individuals.

45 *Findings:* We identified an age-related link between altered basal lipid metabolism in naive CD8⁺

46 T cells and their impaired responsiveness to stimulation, characterized by low proliferative

47 potential and susceptibility to apoptosis. Reversal of the bioenergetic anomalies with lipid-

48 altering drugs, such as rosiglitazone, improved the functional capabilities of naive CD8⁺ T cells in

49 elderly subjects.

50 *Interpretation:* Interventions that favor lipid catabolism may find utility as adjunctive therapies in

51 the elderly to promote vaccine-induced immunity against emerging pathogens or tumors.

52 *Funding:* A full list of the funding sources is detailed in the Acknowledgment section of the

53 manuscript.

54

55

56 **Keywords**

57 Fatty acid, aging, immunosenescence, naive T cells.

58

59 **RESEARCH IN CONTEXT**

60

61 **Evidence before this study**

62 Old subjects are highly susceptible to infections and tumors and usually present with low
63 responses to vaccine. This is mainly due to the age-related loss of primary immune resources, i.e.
64 a quantitative decline of naïve CD8⁺ T cells. Nonetheless, few studies have also underlined,
65 within this cell subset, qualitative defects in elderly subjects.

66 **Added value of this study**

67 Considering the well-demonstrated link between nutrient usage and lymphocyte functions, we
68 characterized the bioenergetics features of old naïve CD8⁺ T cells. Our data show an age-
69 dependent altered basal metabolism in this cell subset, mostly at the levels of fatty acids and
70 mitochondrial functions. These alterations were associated with functional defects which were
71 partially reverted through the use of lipid-lowering strategies.

72 **Implications of all the available evidence**

73 This study highlights the potential role of an altered cellular lipid metabolism in
74 immunosenescence, providing clues to understand the epidemiological profile of emerging
75 infections or tumors and to develop preventive and therapeutic strategies based on metabolic
76 manipulation.

77 **INTRODUCTION**

78
79 Life expectancy has increased considerably over the last century as a consequence of advances in
80 medicine and improved public health systems. However, old age is associated with a high
81 prevalence of chronic diseases and an increased susceptibility to cancer and emerging pathogens,
82 such as SARS-CoV-2 [1]. Age-related deficits in the immune system are thought to play a key
83 role in the development of many pathological conditions [2-4]. Immune aging is characterized by
84 a progressive erosion of the naive CD8⁺ T cell compartment, which impairs *de novo* immune
85 responses against newly encountered antigens [5,6]. In addition to a decline in absolute numbers
86 [7], naive CD8⁺ T cells in elderly individuals exhibit impaired differentiation in response to T cell
87 receptor (TCR)-mediated activation [5].

88
89 A growing body of evidence indicates that lymphocyte metabolism is a key determinant of
90 immune functionality [8-11]. Systemic metabolic disturbances are common in elderly individuals,
91 and increased levels of adipokines and proinflammatory lipid species in particular have been
92 implicated as critical mediators of inflammaging, which is thought to exacerbate many age-related
93 diseases [12]. In this study, we investigated the bioenergetic features of naive CD8⁺ T cells in
94 middle-aged and elderly humans, aiming to establish a link between metabolic disturbances and
95 age-related functional impairments. Naive CD8⁺ T cells displayed specific metabolic
96 abnormalities in elderly people, in particular enhanced lipid influx and storage, accompanied by
97 reduced proliferation and increased susceptibility to apoptosis upon activation. Importantly, these
98 deficits were mitigated in the presence of lipid-altering drugs, opening potential therapeutic
99 avenues to slow the process of immunosenescence.

100 **METHODS**

101

102 **Human subjects and samples**

103 Two groups of healthy volunteers were enrolled in this study: (i) middle-aged Caucasians (19 to
104 55 years old; median: 39); and (ii) elderly Caucasians (65 to 95 years old; median: 82).

105 Individuals with malignancies, acute diseases, or severe chronic diseases, such as atherosclerosis,
106 congestive heart failure, poorly controlled diabetes mellitus, renal or hepatic disease, various
107 inflammatory conditions, or chronic obstructive pulmonary disease, as well as individuals on
108 immunosuppressive therapy, were excluded from the study. PBMCs were isolated from venous
109 blood samples via density gradient centrifugation according to standard protocols and
110 cryopreserved in complete medium supplemented with dimethyl sulfoxide (DMSO; 10% v/v;
111 Sigma-Aldrich) and fetal calf serum (FCS; 20% v/v; Sigma-Aldrich). Complete medium (R+)
112 consisted of RPMI 1640 supplemented with non-essential amino acids (1% v/v),
113 penicillin/streptomycin (100 U/mL), L-glutamine (2 mM), and sodium pyruvate (1 mM) (all from
114 Thermo Fisher Scientific).

115

116 **Flow cytometry and cell sorting**

117 PBMCs were stained for surface markers using combinations of the following directly conjugated
118 monoclonal antibodies: anti-CCR7–BV650 (clone 3D12; BD Biosciences), anti-CCR7–PE–Cy7
119 (clone 3D12; BD Biosciences), anti-CD3–BV605 (clone SK7; BD Biosciences), anti-CD8–APC
120 (clone RPA-T8; BD Biosciences), anti-CD8–APC–Cy7 (clone SK1; BD Biosciences), anti-CD8–
121 FITC (clone RPA-T8; BD Biosciences), anti-CD27–AF700 (clone O323; BioLegend), anti-
122 CD27–PE (clone M-T271; BD Biosciences), anti-CD45RA–ECD (clone 2H4LDH11LDB9;
123 Beckman Coulter), anti-CD45RA–PerCP–Cy5.5 (clone HI100; eBioscience), anti-CD45RA–V450
124 (clone HI100; BD Biosciences), anti-CD49b–PE–Cy7 (clone 9F10; BioLegend), anti-CD57–

125 Pacific Blue (clone HCD57; BioLegend), and anti-CD95–FITC (clone DX2; BD Biosciences).
126 Naive CD8⁺ T cells were defined as CD3⁺ CD8⁺ CD27⁺ CD45RA⁺ CCR7⁺ in most experiments
127 and further identified as CD49b⁻ CD57⁻ CD95⁻ for gene expression studies and intracellular
128 measurements of T-bet. Non-viable cells were eliminated from the analysis using LIVE/DEAD
129 Fixable Aqua (Thermo Fisher Scientific). Intracellular stains were performed using anti-T-bet–
130 eFluor660 (clone 4B10; eBioscience) in conjunction with a Transcription Factor Buffer Set (BD
131 Biosciences). Samples were acquired using an LSR Fortessa or a FACSCanto II (BD
132 Biosciences). Naive CD8⁺ T-cells were flow-sorted using a FACS Aria II (BD Biosciences). Data
133 were analyzed using FACSDiva software version 7 (BD Biosciences) and/or FlowJo software
134 version 10 (FlowJo LLC).

135

136 **Proliferation assays**

137 PBMCs were labeled with Cell Proliferation Dye (CPD) eFluor450 (Thermo Fisher Scientific)
138 and stimulated for 4 days with plate-bound anti-CD3 (clone OKT3; Thermo Fisher Scientific) in
139 the absence or presence of CTAB (1 μM; Sigma-Aldrich). In some experiments, cells were
140 precultured in AIM-V medium (Thermo Fisher Scientific) supplemented with bovine serum
141 albumin (BSA; 10% v/v; Sigma-Aldrich) for 1 day in the absence or presence of palmitic acid
142 (300 μM; Sigma-Aldrich), and in other experiments, cells were precultured in AIM-V medium
143 (Thermo Fisher Scientific) without BSA supplementation for 2 days in the absence or presence of
144 rosiglitazone (40 μM; Sigma-Aldrich). Proliferation was measured using flow cytometry to
145 quantify the dilution of CPD.

146

147 **Activation assays**

148 PBMCs were stimulated for 24 hr with plate-bound anti-CD3 (clone OKT3; Thermo Fisher
149 Scientific) in the absence or presence of fenofibrate (50 μM; Sigma-Aldrich) or rosiglitazone (40

150 μM ; Sigma-Aldrich). The expression of the standard activation markers CD69 and CD134
151 (OX40) was quantified on the cell surface using anti-CD69–FITC (clone L78; BD Biosciences)
152 and anti-CD134–BV711 (clone ACT35; BD Biosciences). Intracellular staining for activated
153 caspase-3, used as marker of susceptibility to apoptosis upon activation, was performed using
154 anti-active caspase-3–PE (clone C92-605; BD Biosciences) in conjunction with a
155 Cytotfix/Cytoperm Fixation/Permeabilization Solution Kit (BD Biosciences).

156

157 **Metabolism assays**

158 To determine glucose uptake, PBMCs were incubated for 20 min at 37°C in phosphate-buffered
159 saline (PBS) containing 2'-(N-(7-nitrobenz-2-oxa-1,3-diazol-4-yl)amino)-2-deoxyglucose (2-
160 NBDG; 50 μM ; Thermo Fisher Scientific). To determine FA uptake, PBMCs were incubated for
161 20 min at 37°C in PBS containing 4,4-difluoro-5,7-dimethyl-4-bora-3a,4a-diaza-s-indacene-3-
162 hexadecanoic acid (BODIPY FL C16; 1 μM ; Thermo Fisher Scientific). To determine neutral
163 lipid content, PBMCs were incubated for 20 min at 37°C in PBS containing 4,4-difluoro-
164 1,3,5,7,8-pentamethyl-4-bora-3a,4a-diaza-s-indacene (BODIPY 493/503; 10 μM ; Thermo Fisher
165 Scientific). To determine mitochondrial mass, PBMCs were incubated for 30 min at 37°C in R+
166 containing Mitotracker Deep Red (500 nM; Thermo Fisher Scientific). To determine
167 mitochondrial membrane potential, PBMCs were incubated for 30 min at 37°C in R+ containing
168 tetramethylrhodamine, methyl ester, perchlorate (TMRM; 25 nM; Thermo Fisher Scientific). To
169 determine mTOR activity, PBMCs were incubated for 10 min at 37°C in Cytotfix Fixation Buffer
170 (BD Biosciences), washed, incubated for 30 min at 4°C in Phosflow Perm Buffer III (BD
171 Biosciences), washed again, and stained for 1 hr at room temperature with anti-pS6–Pacific Blue
172 (clone D57.2.2E; Cell Signaling Technology).

173

174 **Peptides and tetramers**

175 All peptides were synthesized at >95% purity (BioSynthesis Inc.). The EV20 peptide
176 (YTAAEELAGIGILTVILGVL, Melan-A_{21-40/A27L}) was used for *in vitro* priming studies.
177 Fluorochrome-labeled tetrameric complexes of HLA-A*02:01–EV10 (ELAGIGILTV, Melan-
178 A_{26-35/A27L}) were generated in-house as described previously [13].

179

180 ***In vitro* priming of antigen-specific CD8⁺ T cells**

181 Naive precursors specific for HLA-A2–EV10 were primed *in vitro* using an accelerated dendritic
182 cell (DC) coculture protocol as described previously [9,14,15]. Briefly, thawed PBMCs were
183 resuspended at 5×10^6 cells/well in AIM-V medium (Thermo Fisher Scientific) supplemented
184 with Flt3 ligand (Flt3L; 50 ng/ml; R&D Systems) in the absence or presence of rosiglitazone (40
185 μ M; Sigma-Aldrich) or IL-7 (20 ng/mL; R&D Systems). After 24 hr (day 1), the Melan-A peptide
186 EV20 (1 μ M) was added to the cultures, and DC maturation was induced using a standard
187 cocktail of inflammatory cytokines, incorporating IL-1 β (10 ng/mL), IL-7 (0.5 ng/mL),
188 prostaglandin E2 (PGE2; 1 μ M), and TNF (1,000 U/mL) (all from R&D Systems), or ssRNA40
189 (TLR8L; 0.5 μ g/mL; InvivoGen). The cultures were supplemented on day 2 with FCS (10% v/v;
190 Sigma-Aldrich). Medium was replaced every 3 days thereafter with fresh R+ containing FCS
191 (10% v/v; Sigma-Aldrich). Antigen-specific CD8⁺ T cells were characterized via flow cytometry
192 on day 10.

193

194 **RNA extraction and qPCR analysis**

195 PBMCs were activated for 5 hr with plate-bound anti-CD3 (clone OKT3; Thermo Fisher
196 Scientific). RNA was extracted from flow-sorted naive CD8⁺ T cells (n = 300 per condition)
197 using a NucleoSpin RNA XS Kit (Macherey-Nagel), and cDNA was synthesized using Reverse
198 Transcription Master Mix (Fluidigm). Specific targets were amplified using PreAmp Master Mix
199 (Fluidigm). Gene expression was assessed using a BioMark HD System (Fluidigm) with

200 EvaGreen Supermix (Bio-Rad). RNA expression levels were calculated using the $2^{-\Delta\Delta CT}$ method
201 with reference to a housekeeping gene (human 18S) [16].

202

203 **Statistics**

204 Univariate statistical analyses were performed using nonparametric tests in Prism software
205 version 8 (GraphPad Software Inc.). Significance was assigned at $p < 0.05$.

206

207 **Study Approval**

208 Ethical approval was granted by the Comité de Protection des Personnes of the Pitié Salpêtrière
209 Hospital (Paris, France). All volunteers provided written informed consent in accordance with the
210 Declaration of Helsinki.

211

212 **RESULTS**

213

214 **Naive CD8⁺ T cells in the elderly exhibit altered basal activation status and proliferative**
215 **capacity**

216 We previously demonstrated that naïve CD8⁺ T cells from elderly individuals generate, upon
217 encountering their cognate antigen, qualitatively altered effector cells characterized by a skewed
218 differentiation status and a poor cytotoxic potential [5]. To better characterize this phenomenon,
219 we compared the activation profiles of naïve CD8⁺ T cells in middle-aged and elderly individuals,
220 mimicking antigen-driven signals with plate-bound anti-CD3. No age-related differences in
221 activation *per se* were detected 24 hr after stimulation, as determined by measuring the
222 upregulation of CD69 and CD134 (Figure 1a). Despite these phenotypic similarities, naïve CD8⁺
223 T cells from elderly individuals proliferated to a lower extent than naïve CD8⁺ T cells from
224 middle-aged individuals in response to stimulation with plate-bound anti-CD3 (Figure 1b),
225 consistent with their poor expansion upon priming [5]. Susceptibility to apoptosis upon activation
226 was also more commonly observed among activated naïve CD8⁺ T cells from elderly *versus*
227 middle-aged individuals, as determined by the intracellular expression of active caspase-3, known
228 to be a central element of the apoptotic pathway (Figure 1c). Of note, the proliferative capacity
229 and susceptibility to apoptosis of naïve CD8⁺ T cells upon stimulation were inversely correlated,
230 irrespective of age (Figure 1d).

231 Unstimulated naïve CD8⁺ T cells from elderly individuals expressed CD134 more commonly than
232 unstimulated naïve CD8⁺ T cells from middle-aged individuals, suggesting increased levels of
233 basal activation with advanced age (Figure 1a). To consolidate this observation, we measured the
234 expression of T-bet, which is classically upregulated in response to activation. The basal
235 expression frequencies of T-bet mirrored the basal expression frequencies of CD134 (Figure 1e).
236 Equivalent results were obtained using a more stringent definition of naïve CD8⁺ T cells (Figures

237 S1a and S1b), which excluded phenotypically similar memory CD8⁺ T cells [17]. The basal
238 expression frequency of T-bet also correlated directly with the activation-induced expression
239 frequency of active caspase-3 among naive CD8⁺ T cells (Figure 1f).

240 Collectively, these data indicate that the deficit in proliferation of old naive CD8⁺ T cells is
241 associated with higher basal activation status and susceptibility to apoptosis, despite a largely
242 unaltered early response to activation.

243 244 **Naive CD8⁺ T cells in the elderly are metabolically distinct**

245 Signals transduced via the TCR elicit an mTOR-driven metabolic switch that supports the
246 function and the viability of activated naive CD8⁺ T cells [9]. We therefore assessed mTOR
247 activity in parallel by quantifying phospho-S6 (pS6). In line with the comparable activation
248 profiles, naive CD8⁺ T cells in middle-aged and elderly individuals upregulated mTOR activity to
249 a similar extent after stimulation with plate-bound anti-CD3 (Figure 2a). To extend these findings,
250 we measured the expression of metabolism-related genes, comparing unstimulated and activated
251 naive CD8⁺ T cells (Figure 2b). Genes encoding various enzymes involved in glycolysis were
252 upregulated similarly in flow-sorted naive CD8⁺ T cells from middle-aged and elderly individuals
253 after stimulation with plate-bound anti-CD3. In contrast, genes associated with lipid metabolism
254 or signaling pathways involved in metabolic regulation were not generally upregulated in
255 response to stimulation, with the exception of *MYC*, which was overexpressed in activated naive
256 CD8⁺ T cells, irrespective of age. Genes that play a critical role in the metabolic switch were also
257 overexpressed in activated naive CD8⁺ T cells, irrespective of age, with the exception of *HIF1*
258 and *RPS6KB1*, which were upregulated to a greater extent in activated naive CD8⁺ T cells from
259 middle-aged *versus* elderly individuals. This dataset indicates a rather intact although suboptimal
260 metabolic switch, with a physiological mTOR activation, in naive CD8⁺ T cells of elderly
261 subjects upon TCR ligation.

262 To explore the age-related homeostatic change in more detail, i.e. prior to activation, we
263 investigated the biochemical features of quiescent naive CD8⁺ T cells. These cells are present at
264 very low frequencies in elderly donors [5], posing challenges to the determination of metabolic
265 fluxes, for instance using standard approaches like Seahorse technology. We therefore engaged in
266 the characterization of different metabolic pathways using flow cytometry and gene expression
267 profiles. Glycolysis is the main metabolic pathway that supports the activation of naive CD8⁺ T
268 cells [9,18]. We found no significant differences in basal glucose uptake between unstimulated
269 naive CD8⁺ T cells from middle-aged individuals and unstimulated naive CD8⁺ T cells from
270 elderly individuals (Figure 3a). Moreover, we found similar basal expression levels of glycolysis-
271 related genes, with the exception of *HK2*, which was overexpressed in unstimulated naive CD8⁺ T
272 cells from middle-aged *versus* elderly individuals (Figure 3b). This gene encodes a selectively
273 regulated isoform of hexokinase [19], which catalyzes glucose phosphorylation, and is usually
274 induced in response to stimulation via the TCR [19,20]. Interestingly, fatty acid (FA) uptake was
275 decreased among unstimulated naive CD8⁺ T cells from middle-aged *versus* elderly individuals
276 (Figure 3c), but this difference was not associated with significant changes in the expression
277 levels of genes encoding various enzymes involved in FA oxidation (FAO) or FA synthesis
278 (FAS). However, we noted that *DGATI*, which encodes diacylglycerol O-acyltransferase 1, a key
279 enzyme involved in the storage of FAs as triacylglycerol (TAG), was expressed at lower levels,
280 although not statistically significant, in unstimulated naive CD8⁺ T cells from middle-aged *versus*
281 elderly individuals (Figure 3d).

282 In addition, we observed that unstimulated naive CD8⁺ T cells from middle-aged individuals
283 stored lower amounts of neutral lipids (NLs) than unstimulated naive CD8⁺ T cells from elderly
284 individuals (Figure 4a). In further experiments, we assessed the basal expression levels of various
285 genes encoding transcription factors involved in metabolic regulation. Similar patterns of
286 expression were observed in unstimulated naive CD8⁺ T cells, irrespective of age, with the

287 exception of *ID2*, which was expressed at lower levels in unstimulated naive CD8⁺ T cells from
288 middle-aged *versus* elderly individuals (Figure 4b). *ID2* is involved in metabolic adaptation
289 [21,22] and promotes lipid storage via the downmodulation of *PGC-1 α* [22], which enhances
290 FAO and inhibits TAG synthesis [23]. Moreover, *ID2* promotes an overall increase in
291 mitochondrial membrane potential ($\Delta\Psi$ M), without affecting mitochondrial biogenesis or, by
292 extension, mitochondrial mass [21]. In line with these known functions, $\Delta\Psi$ M was lower in
293 unstimulated naive CD8⁺ T cells from middle-aged *versus* elderly individuals (Figure 4c),
294 whereas mitochondrial mass was largely unaffected by age (Figure 4d). We also noted a direct
295 correlation between $\Delta\Psi$ M and the frequency of unstimulated naive CD8⁺ T cells that expressed T-
296 bet, suggesting a link with the loss of quiescence (Figure S2).
297 Collectively, these data revealed an age-related shift in the basal metabolic properties of naive
298 CD8⁺ T cells, typified by a supranormal $\Delta\Psi$ M and high levels of FA uptake and NL storage.

299

300 **Naive CD8⁺ T cells in the elderly can be reinvigorated with lipid-altering drugs**

301 While FAs are indispensable for cellular lifespan, and in particular for the formation of cell
302 membranes, their excessive levels can have negative effects on cell physiology. T cell
303 homeostasis and viability can for instance be affected by high levels of FAs [24,25]. We therefore
304 assessed the potential link between the functional properties of old naïve T cells and their altered
305 lipid metabolism. We first observed direct correlations between the frequency of unstimulated
306 naive CD8⁺ T cells that expressed active caspase-3 and basal levels of FA uptake (Figure 5a) and
307 NL content (Figure 5b). To determine the biological relevance of these associations, we treated
308 naive CD8⁺ T cells with rosiglitazone, a drug known to foster lipid catabolism by activating
309 triglyceride lipase [26] and preventing the conversion of FAs into NLs [27]. Exposure to
310 rosiglitazone in serum starvation conditions boosted indeed NL catabolism in naive CD8⁺ T cells,
311 as observed with a decrease of cellular NL content (Figure 5c). Pretreatment with rosiglitazone

312 reduced activation-induced active caspase-3 expression among naive CD8⁺ T cells of elderly
313 subjects (Figure 5d). Similar results were obtained using fenofibrate, which induces lipid
314 catabolism by enhancing FAO (Figure S3).

315 With regards to proliferative capacity, naive CD8⁺ T cells from elderly individuals proliferated to
316 a greater extent after serum starvation, and the addition of rosiglitazone further enhanced these
317 activation-induced proliferative responses (Figure 5e). To assess the potential relevance of these
318 findings in the context of antigen-driven immune responses, we used a previously established *in*
319 *vitro* model to prime naive CD8⁺ T cells specific for EV10, a melanoma-derived HLA-A2
320 restricted epitope, starting from PBMCs of melanoma-naïve individuals. We developed and have
321 used this assay to study human CD8⁺ T cell priming [5]. As expected from the proliferation data,
322 EV10-specific CD8⁺ T cells from middle-aged individuals expanded to a greater extent than
323 EV10-specific CD8⁺ T cells from elderly individuals (Figure 5f), and preincubation with
324 rosiglitazone consistently enhanced the expansion of EV10-specific CD8⁺ T cells from elderly
325 individuals (Figure 5g).

326 Collectively, these data indicate that age-related functional deficits associated with abnormal lipid
327 metabolism and greater levels of basal activation in the naive CD8⁺ T cell compartment may be,
328 at least in part, reversed in the presence of rosiglitazone, opening potentially useful therapeutic
329 approaches to enhance immune reactivity against newly encountered antigens in the elderly.

330

331 **DISCUSSION**

332 A detailed understanding of age-related deficits in the naive T cell compartment is essential for
333 the rational development of immunotherapies and vaccines that protect elderly individuals from
334 emerging threats. We found that naive CD8⁺ T cells in elderly individuals were susceptible to
335 apoptosis and proliferated suboptimally in response to stimulation. These abnormalities were
336 associated with enhanced levels of basal activation, measured in terms of $\Delta\Psi\text{M}$ and the *ex vivo*
337 expression frequencies of T-bet and CD134.

338

339 Recent studies have shown that metabolic processes govern the behavior of T cells [9,18,29,30].
340 In the naive CD8⁺ T cell compartment, autophagy and glycolysis are typically upregulated in
341 response to activation [9,31,32], whereas homeostatic energy requirements are fulfilled primarily
342 via FAO [11,33-36]. We observed that, at rest, naive CD8⁺ T cells in the elderly displayed
343 abnormally high levels of FA uptake and stored abnormally high amounts of NLs. In line with
344 previous reports showing that high levels of intracellular lipids may be toxic [9,24,37], we found
345 that active caspase-3 expression correlated directly with FA uptake and NL content in the naive
346 CD8⁺ T cell compartment. Lipids are essential for T cell activation and proliferation [28].
347 Excessively high amounts of intracellular lipids can nonetheless impair T cell proliferation and
348 viability [38-40]. Accordingly, we found that activation-induced initiation of the apoptotic
349 pathway was reduced by interventions enhancing lipid clearance in naive CD8⁺ T cells. Of note,
350 NLs *per se* are not toxic. The conversion of FAs into NLs therefore most likely protects against
351 lipotoxicity under homeostatic conditions [24].

352

353 The heightened basal activation status of naive CD8⁺ T cells in elderly individuals seemed to be
354 sustained energetically by increased mitochondrial activity, given that T-bet expression correlated
355 directly with $\Delta\Psi\text{M}$. Inflammation is closely linked with metabolic dysregulation in the elderly

356 [41]. High levels of circulating proinflammatory cytokines and lipids are common features of
357 advanced age and may contribute to the disruption of cellular quiescence. Moreover,
358 hematopoietic progenitor cells in elderly individuals are often metabolically active, and this
359 characteristic may be heritable [42]. Increased rates of homeostatic proliferation are required to
360 maintain naïve CD8⁺ T cell numbers in the elderly [43], and the predominant energetic pathway
361 that supports this process is thought to be FAO [44,45]. It is therefore plausible that high basal
362 levels of FA uptake and NL storage constitute a bioenergetic pattern that favors homeostatic
363 proliferation.

364

365 Aging is characterized by profound metabolic perturbations [46], including increased lipogenesis
366 [47] and reduced lipolysis [48], leading to higher systemic levels of free FAs and TAG [41,49].
367 The combination of a homeostatic environment and high systemic levels of proinflammatory
368 cytokines and lipids may potentially underlie the altered metabolism and functional deficits that
369 characterize naïve CD8⁺ T cells in the elderly. A key finding of our study was the observation that
370 rosiglitazone, known to foster lipid catabolism, can improve these abnormalities, and enhance old
371 naïve T cell priming. The experimental model we exploited (i.e. *in vitro* priming of melanoma-
372 specific naïve CD8⁺ T cells) was previously shown to mimic *in vivo* responses in both mice and
373 humans [5,50,51]. The positive effect of rosiglitazone in this model is an encouraging result from
374 a translational perspective. Of note, a recent study showed that treatment with this drug was
375 associated with a delay of age-associated metabolic disease and extend longevity in old mice
376 [52]. Although rosiglitazone, initially licensed for the treatment of diabetes mellitus, was
377 eventually withdrawn due several side effects, it serves as proof of concept that inducing lipolysis
378 prior to T-cell priming could be beneficial in the context of vaccinations and immunotherapy,
379 akin to recent data showing that increased FAO can improve the development and the quality of
380 effector CD8⁺ T cells [9,53-55]. Further studies are therefore warranted to screen whether other

381 lipid-altering drugs may be useful adjunctive therapies to enhance adaptive immune responses
382 against previously unencountered antigens, particularly in elderly individuals, who often respond
383 poorly to vaccination and remain vulnerable to emerging pathogens, such as seasonal influenza
384 viruses and SARS-CoV-2.
385

386 **Contributors**

387 F.N., R.G., and V.A. conceptualized the project; F.N., M.P.C.P., L.P., E.Ga., V.F., and J.J.F.
388 performed experiments and analyzed data; M.D., E.C., H.V., E.Go., S.L.L., D.A.P., A.T., and J.B.
389 provided critical resources; F.N., J.F.F., R.G., and V.A. drafted the manuscript; F.N., D.A.P.,
390 A.C., R.G., and V.A. edited the manuscript; D.A.P., A.T., A.C., and V.A. acquired funds to
391 support the work. All authors contributed intellectually and approved the manuscript.

392

393 **Declaration of Competing Interests**

394 The authors declare no conflict of interest.

395

396 **Acknowledgements**

397 We thank Simone Candioli and Silvio Spatocco (University of Ferrara, Italy), Irene Bonazzi and
398 Ilaria Signoretto (University of Padua, Italy), and Alain Savenay (AP-HP, Paris, France) for
399 technical assistance, Mario Pende (Institut Necker-Enfants Malades, Paris, France) for helpful
400 discussions, and Veronique Morin and Rima Zoorob (INSERM U1135, Paris, France) and Silvia
401 Menegatti and Lars Rogge (Institut Pasteur, Paris, France) for assistance with gene expression
402 analyses. This work was supported by the Agence National de la Recherche (ANR-14-CE14-
403 0030-01) and the Université Franco-Italienne/Università Italo-Francese (Galileo Project G10-718;
404 PHC Galilee Project 39582TJ). Core provision of the FACSCanto II was funded by the University
405 of Ferrara (Bando per l'acquisizione di strumenti per la ricerca di ateneo-2015). D.A.P. was
406 supported by a Wellcome Trust Senior Investigator Award (100326/Z/12/Z).

407

408 **Data Sharing**

409 Data collected for the study will be made available upon reasonable request made to the
410 corresponding authors FN and VA.

411 **REFERENCES**

- 412 [1] Nicoli F, Solis-Soto MT, Paudel D, et al. Age-related decline of de novo T cell
413 responsiveness as a cause of COVID-19 severity. *Geroscience*. 2020; **42**: 1015-9.
- 414 [2] Dorshkind K, Swain S. Age-associated declines in immune system development and
415 function: causes, consequences, and reversal. *Curr Opin Immunol*. 2009; **21**: 404-7.
- 416 [3] Ventura MT, Casciaro M, Gangemi S, Buquicchio R. Immunosenescence in aging:
417 between immune cells depletion and cytokines up-regulation. *Clin Mol Allergy*. 2017; **15**: 21.
- 418 [4] Fulop T, Larbi A, Dupuis G, et al. Immunosenescence and Inflamm-Aging As Two Sides
419 of the Same Coin: Friends or Foes? *Front Immunol*. 2017; **8**: 1960.
- 420 [5] Briceno O, Lissina A, Wanke K, et al. Reduced naive CD8(+) T-cell priming efficacy in
421 elderly adults. *Aging Cell*. 2016; **15**: 14-21.
- 422 [6] Nikolich-Zugich J. Aging of the T cell compartment in mice and humans: from no naive
423 expectations to foggy memories. *J Immunol*. 2014; **193**: 2622-9.
- 424 [7] Wertheimer AM, Bennett MS, Park B, et al. Aging and cytomegalovirus infection
425 differentially and jointly affect distinct circulating T cell subsets in humans. *J Immunol*. 2014;
426 **192**: 2143-55.
- 427 [8] Palmer CS, Ostrowski M, Balderson B, Christian N, Crowe SM. Glucose metabolism
428 regulates T cell activation, differentiation, and functions. *Front Immunol*. 2015; **6**: 1.
- 429 [9] Nicoli F, Papagno L, Frere JJ, et al. Naive CD8(+) T-Cells Engage a Versatile Metabolic
430 Program Upon Activation in Humans and Differ Energetically From Memory CD8(+) T-Cells.
431 *Front Immunol*. 2018; **9**: 2736.
- 432 [10] Nicoli F. Angry, Hungry T-Cells: How Are T-Cell Responses Induced in Low Nutrient
433 Conditions? *Immunometabolism*. 2020; **2**: e200004.
- 434 [11] Almeida L, Lochner M, Berod L, Sparwasser T. Metabolic pathways in T cell activation
435 and lineage differentiation. *Semin Immunol*. 2016; **28**: 514-24.
- 436 [12] Baylis D, Bartlett DB, Patel HP, Roberts HC. Understanding how we age: insights into
437 inflammaging. *Longev Healthspan*. 2013; **2**: 8.
- 438 [13] Price DA, Brenchley JM, Ruff LE, et al. Avidity for antigen shapes clonal dominance in
439 CD8+ T cell populations specific for persistent DNA viruses. *J Exp Med*. 2005; **202**: 1349-61.
- 440 [14] Lissina A, Briceno O, Afonso G, et al. Priming of Qualitatively Superior Human Effector
441 CD8+ T Cells Using TLR8 Ligand Combined with FLT3 Ligand. *J Immunol*. 2016; **196**: 256-63.
- 442 [15] Alanio C, Nicoli F, Sultanik P, et al. Bystander hyperactivation of preimmune CD8+ T
443 cells in chronic HCV patients. *Elife*. 2015; **4**: 1-20.
- 444 [16] Nicoli F, Gallerani E, Sforza F, et al. The HIV-1 Tat protein affects human CD4+ T-cell
445 programming and activation, and favors the differentiation of naive CD4+ T cells. *AIDS*. 2018; **32**:
446 575-81.
- 447 [17] Pulko V, Davies JS, Martinez C, et al. Human memory T cells with a naive phenotype
448 accumulate with aging and respond to persistent viruses. *Nat Immunol*. 2016; **17**: 966-75.
- 449 [18] Zhang L, Romero P. Metabolic Control of CD8(+) T Cell Fate Decisions and Antitumor
450 Immunity. *Trends Mol Med*. 2018; **24**: 30-48.
- 451 [19] Tan H, Yang K, Li Y, et al. Integrative Proteomics and Phosphoproteomics Profiling
452 Reveals Dynamic Signaling Networks and Bioenergetics Pathways Underlying T Cell Activation.
453 *Immunity*. 2017; **46**: 488-503.

- 454 [20] Lis P, Dylag M, Niedzwiecka K, et al. The HK2 Dependent "Warburg Effect" and
455 Mitochondrial Oxidative Phosphorylation in Cancer: Targets for Effective Therapy with 3-
456 Bromopyruvate. *Molecules*. 2016; **21**.
- 457 [21] Zhang Z, Rahme GJ, Chatterjee PD, Havrda MC, Israel MA. ID2 promotes survival of
458 glioblastoma cells during metabolic stress by regulating mitochondrial function. *Cell Death Dis*.
459 2017; **8**: e2615.
- 460 [22] Hou TY, Ward SM, Murad JM, Watson NP, Israel MA, Duffield GE. ID2 (inhibitor of
461 DNA binding 2) is a rhythmically expressed transcriptional repressor required for circadian clock
462 output in mouse liver. *J Biol Chem*. 2009; **284**: 31735-45.
- 463 [23] Morris EM, Meers GM, Booth FW, et al. PGC-1alpha overexpression results in increased
464 hepatic fatty acid oxidation with reduced triacylglycerol accumulation and secretion. *Am J*
465 *Physiol Gastrointest Liver Physiol*. 2012; **303**: G979-92.
- 466 [24] de Jong AJ, Kloppenburg M, Toes RE, Ioan-Facsinay A. Fatty acids, lipid mediators, and
467 T-cell function. *Front Immunol*. 2014; **5**: 483.
- 468 [25] Nicoli F, Paul S, Appay V. Harnessing the Induction of CD8+ T-Cell Responses Through
469 Metabolic Regulation by Pathogen-Recognition-Receptor Triggering in Antigen Presenting Cells.
470 *Frontiers in Immunology*. 2018; **9**.
- 471 [26] Kershaw EE, Schupp M, Guan HP, Gardner NP, Lazar MA, Flier JS. PPARgamma
472 regulates adipose triglyceride lipase in adipocytes in vitro and in vivo. *Am J Physiol Endocrinol*
473 *Metab*. 2007; **293**: E1736-45.
- 474 [27] Askari B, Kanter JE, Sherrid AM, et al. Rosiglitazone inhibits acyl-CoA synthetase
475 activity and fatty acid partitioning to diacylglycerol and triacylglycerol via a peroxisome
476 proliferator-activated receptor-gamma-independent mechanism in human arterial smooth muscle
477 cells and macrophages. *Diabetes*. 2007; **56**: 1143-52.
- 478 [28] Angela M, Endo Y, Asou HK, et al. Fatty acid metabolic reprogramming via mTOR-
479 mediated inductions of PPARgamma directs early activation of T cells. *Nat Commun*. 2016; **7**:
480 13683.
- 481 [29] Gubser PM, Bantug GR, Razik L, et al. Rapid effector function of memory CD8+ T cells
482 requires an immediate-early glycolytic switch. *Nat Immunol*. 2013; **14**: 1064-72.
- 483 [30] O'Neill LA, Kishton RJ, Rathmell J. A guide to immunometabolism for immunologists.
484 *Nat Rev Immunol*. 2016; **16**: 553-65.
- 485 [31] Arnold CR, Pritz T, Brunner S, et al. T cell receptor-mediated activation is a potent
486 inducer of macroautophagy in human CD8(+)/CD28(+) T cells but not in CD8(+)/CD28(-) T cells.
487 *Exp Gerontol*. 2014; **54**: 75-83.
- 488 [32] Whang MI, Tavares RM, Benjamin DI, et al. The Ubiquitin Binding Protein TAX1BP1
489 Mediates Autophagosome Induction and the Metabolic Transition of Activated T Cells. *Immunity*.
490 2017; **46**: 405-20.
- 491 [33] O'Sullivan D, van der Windt GJ, Huang SC, et al. Memory CD8(+) T cells use cell-
492 intrinsic lipolysis to support the metabolic programming necessary for development. *Immunity*.
493 2014; **41**: 75-88.
- 494 [34] Green WD, Beck MA. Obesity altered T cell metabolism and the response to infection.
495 *Curr Opin Immunol*. 2017; **46**: 1-7.
- 496 [35] Pearce EL, Walsh MC, Cejas PJ, et al. Enhancing CD8 T-cell memory by modulating
497 fatty acid metabolism. *Nature*. 2009; **460**: 103-7.

- 498 [36] Raud B, McGuire PJ, Jones RG, Sparwasser T, Berod L. Fatty acid metabolism in CD8(+)
499 T cell memory: Challenging current concepts. *Immunol Rev.* 2018; **283**: 213-31.
- 500 [37] Zurier RB, Rossetti RG, Seiler CM, Laposata M. Human peripheral blood T lymphocyte
501 proliferation after activation of the T cell receptor: effects of unsaturated fatty acids.
502 *Prostaglandins Leukot Essent Fatty Acids.* 1999; **60**: 371-5.
- 503 [38] Takahashi HK, Cambiaghi TD, Luchessi AD, et al. Activation of survival and apoptotic
504 signaling pathways in lymphocytes exposed to palmitic acid. *J Cell Physiol.* 2012; **227**: 339-50.
- 505 [39] Fernanda Cury-Boaventura M, Cristine Kanunfre C, Gorjao R, Martins de Lima T, Curi R.
506 Mechanisms involved in Jurkat cell death induced by oleic and linoleic acids. *Clin Nutr.* 2006; **25**:
507 1004-14.
- 508 [40] Howie D, Cobbold SP, Adams E, et al. Foxp3 drives oxidative phosphorylation and
509 protection from lipotoxicity. *JCI Insight.* 2017; **2**: e89160.
- 510 [41] Pararasa C, Ikwuobe J, Shigdar S, et al. Age-associated changes in long-chain fatty acid
511 profile during healthy aging promote pro-inflammatory monocyte polarization via PPARgamma.
512 *Aging Cell.* 2016; **15**: 128-39.
- 513 [42] Fali T, Fabre-Mersseman V, Yamamoto T, et al. Elderly human hematopoietic progenitor
514 cells express cellular senescence markers and are more susceptible to pyroptosis. *JCI Insight.*
515 2018; **3**.
- 516 [43] Sauce D, Larsen M, Fastenackels S, et al. Lymphopenia-driven homeostatic regulation of
517 naive T cells in elderly and thymectomized young adults. *J Immunol.* 2012; **189**: 5541-8.
- 518 [44] Chang CH, Curtis JD, Maggi LB, Jr., et al. Posttranscriptional control of T cell effector
519 function by aerobic glycolysis. *Cell.* 2013; **153**: 1239-51.
- 520 [45] Ibitokou SA, Dillon BE, Sinha M, et al. Early Inhibition of Fatty Acid Synthesis Reduces
521 Generation of Memory Precursor Effector T Cells in Chronic Infection. *J Immunol.* 2018; **200**:
522 643-56.
- 523 [46] Bonomini F, Rodella LF, Rezzani R. Metabolic syndrome, aging and involvement of
524 oxidative stress. *Aging Dis.* 2015; **6**: 109-20.
- 525 [47] Kuhla A, Blei T, Jaster R, Vollmar B. Aging is associated with a shift of fatty metabolism
526 toward lipogenesis. *J Gerontol A Biol Sci Med Sci.* 2011; **66**: 1192-200.
- 527 [48] Toth MJ, Tchernof A. Lipid metabolism in the elderly. *Eur J Clin Nutr.* 2000; **54 Suppl 3**:
528 S121-5.
- 529 [49] Mc Auley MT, Mooney KM. Computationally Modeling Lipid Metabolism and Aging: A
530 Mini-review. *Comput Struct Biotechnol J.* 2015; **13**: 38-46.
- 531 [50] Gutjahr A, Papagno L, Nicoli F, et al. The STING ligand cGAMP potentiates the efficacy
532 of vaccine-induced CD8+ T cells. *JCI Insight.* 2019; **4**.
- 533 [51] Gutjahr A, Papagno L, Nicoli F, et al. Cutting Edge: A Dual TLR2 and TLR7 Ligand
534 Induces Highly Potent Humoral and Cell-Mediated Immune Responses. *J Immunol.* 2017; **198**:
535 4205-9.
- 536 [52] Xu L, Ma X, Verma N, et al. PPARgamma agonists delay age-associated metabolic
537 disease and extend longevity. *Aging Cell.* 2020; **19**: e13267.
- 538 [53] Zhang Y, Kurupati R, Liu L, et al. Enhancing CD8+ T Cell Fatty Acid Catabolism within
539 a Metabolically Challenging Tumor Microenvironment Increases the Efficacy of Melanoma
540 Immunotherapy. *Cancer Cell.* 2017; **32**: 377-91 e9.

- 541 [54] Chowdhury PS, Chamoto K, Honjo T. Combination therapy strategies for improving PD-1
542 blockade efficacy: a new era in cancer immunotherapy. *J Intern Med.* 2018; **283**: 110-20.
543 [55] Chowdhury PS, Chamoto K, Kumar A, Honjo T. PPAR-Induced Fatty Acid Oxidation in
544 T Cells Increases the Number of Tumor-Reactive CD8(+) T Cells and Facilitates Anti-PD-1
545 Therapy. *Cancer Immunol Res.* 2018;10.1158/2326-6066.CIR-18-0095.
546
547

548 **FIGURE LEGENDS**

549 **Figure 1. Activation and proliferation of naive CD8⁺ T cells.** (a - c) PBMCs from middle-aged
550 (Mid - 19 to 55 years old) and elderly individuals (Old - 65 to 95 years old) were incubated in the
551 absence or presence of plate-bound anti-CD3. Surface expression of the activation markers CD69
552 and CD134 was measured after 24 hr (a), proliferation was measured after 4 days (b), and active
553 caspase-3 expression was measured after 1 day (c). Left panels: representative flow cytometry
554 profiles. Right panels: data summaries. Data are shown for naive CD8⁺ T cells. Each dot
555 represents one donor. Horizontal lines indicate median values. * $p < 0.05$ (Mann-Whitney U test).
556 (d) Correlation between the frequency of naive CD8⁺ T cells that proliferated after stimulation
557 and the frequency of naive CD8⁺ T cells that expressed active caspase-3 after stimulation. Each
558 dot represents one donor. Significance was determined using Spearman's rank correlation. (e) T-
559 bet expression was measured in unstimulated naive CD8⁺ T cells from middle-aged (Mid) and
560 elderly individuals (Old). Left panel: representative flow cytometry profiles. Right panel: data
561 summary. Each dot represents one donor. Horizontal lines indicate median values. *** $p < 0.001$
562 (Mann-Whitney U test). (f) Correlation between the basal expression frequency of T-bet and the
563 activation-induced expression frequency of active caspase-3 among naive CD8⁺ T cells. Each dot
564 represents one donor. Significance was determined using Spearman's rank correlation.

565

566 **Figure 2. Metabolic switch in the naive CD8⁺ T cell compartment.** (a) PBMCs from middle-
567 aged (Mid) and elderly individuals (Old) were incubated in the absence or presence of plate-
568 bound anti-CD3. Intracellular expression of mTOR activity marker pS6 was measured after 3 hr.
569 Data are shown for naive CD8⁺ T cells. Each dot represents one donor. Horizontal lines indicate
570 median values. * $p < 0.05$ (Mann-Whitney U test). (b) Flow-sorted naive CD8⁺ T cells from
571 middle-aged (n = 4; Mid) and elderly individuals (n = 5; Old) were incubated in the absence or
572 presence of plate-bound anti-CD3. Gene expression levels were measured after 5 hr. Data are

573 shown relative to the unstimulated condition. Bars indicate mean \pm SEM. * $p < 0.05$ (Mann-
574 Whitney U test).

575

576 **Figure 3. Basal metabolism in the naive CD8⁺ T cell compartment.** (a & c) Glucose (a) and
577 FA uptake (c) were measured in unstimulated naive CD8⁺ T cells from middle-aged (Mid) and
578 elderly individuals (Old) by determining the mean fluorescence intensity (MFI) of 2-NBDG, and
579 BODIPY FL C16, respectively. Left panels: representative flow cytometry profiles. Right panels:
580 data summaries. Each dot represents one donor. Horizontal lines indicate median values. * $p <$
581 0.05 (Mann-Whitney U test). (b & d) Expression levels of genes related to glucose (b) and fatty
582 acid metabolism (d) were measured in unstimulated naive CD8⁺ T cells flow-sorted from middle-
583 aged ($n = 5$; Mid) and elderly individuals ($n = 5$; Old). Bars indicate mean \pm SEM. * $p < 0.05$
584 (Mann-Whitney U test).

585

586 **Figure 4. Metabolic control in the naive CD8⁺ T cell compartment.** (a, c & d) NL content (a)
587 and mitochondrial membrane potential (C) and mass (D) were measured in unstimulated naive
588 CD8⁺ T cells from middle-aged (Mid) and elderly individuals (Old) by determining the mean
589 fluorescence intensity (MFI) of BODIPY 493/503, TMRM and Mitotracker Deep Red,
590 respectively. Left panels: representative flow cytometry profiles. Right panels: data summaries.
591 Each dot represents one donor. Horizontal lines indicate median values. * $p < 0.05$, ** $p < 0.01$
592 (Mann-Whitney U test). (b) Expression levels of genes related to signaling pathways involved in
593 metabolic regulation were measured in unstimulated naive CD8⁺ T cells flow-sorted from middle-
594 aged ($n = 5$; Mid) and elderly individuals ($n = 5$; Old). Bars indicate mean \pm SEM. * $p < 0.05$
595 (Mann-Whitney U test).

596

597 **Figure 5. Effects of lipid-altering drugs in the naive CD8⁺ T cell compartment. (a & b)**

598 Correlations between the frequency of unstimulated naive CD8⁺ T cells that expressed active
599 caspase-3 and basal levels of FA uptake (a) and NL content (b) measured by determining the
600 mean fluorescence intensity (MFI) of BODIPY FL C16 and BODIPY 493/503, respectively. Each
601 dot represents one donor. Significance was determined using Spearman's rank correlation. (c)
602 PBMCs were preincubated for 2 days in serum-free medium in the absence or presence of
603 rosiglitazone (Ros). NL content was measured in naive CD8⁺ T cells by determining the mean
604 fluorescence intensity (MFI) of BODIPY 493/503. Flow cytometry profiles are representative of
605 five independent experiments. (d) PBMCs from elderly individuals (n = 8) were stimulated with
606 plate-bound anti-CD3 in the absence or presence of rosiglitazone (Ros). Active caspase-3
607 expression was measured after 24 hr. Data are shown for naive CD8⁺ T cells. Left panel:
608 representative flow cytometry profiles. Right panel: data summary. Bars indicate mean ± SEM. *
609 p < 0.05 (Wilcoxon signed rank test). (e) PBMCs from elderly individuals were preincubated for
610 2 days in serum-free medium in the absence or presence of rosiglitazone (Ros) and stimulated
611 with plate-bound anti-CD3. Proliferation was measured after 4 days. Data are shown for naive
612 CD8⁺ T cells. Left panel: representative flow cytometry profiles. Right panel: data summary.
613 Each dot represents one donor. Horizontal lines indicate median values. * p < 0.05, ** p < 0.01
614 (Mann-Whitney *U* test). (f) Percentage of tetramer⁺ EV10-specific CD8⁺ T cells expanded for 10
615 days in the presence of Flt3 ligand and a cocktail of inflammatory cytokines. Each dot represents
616 one donor. Horizontal lines indicate median values. * p < 0.05 (Mann-Whitney *U* test). (g)
617 Percentage of tetramer⁺ EV10-specific CD8⁺ T cells of elderly individuals expanded for 10 days
618 in the presence of Flt3 ligand and a cocktail of inflammatory cytokines after preincubation for 2
619 days in the absence or presence of rosiglitazone (Ros). Left panel: representative flow cytometry
620 profiles. Right panel: data summary. Each dot represents one donor. Horizontal lines indicate
621 median values. * p < 0.05 (Wilcoxon signed rank test). NT: not treated.

Figure 1

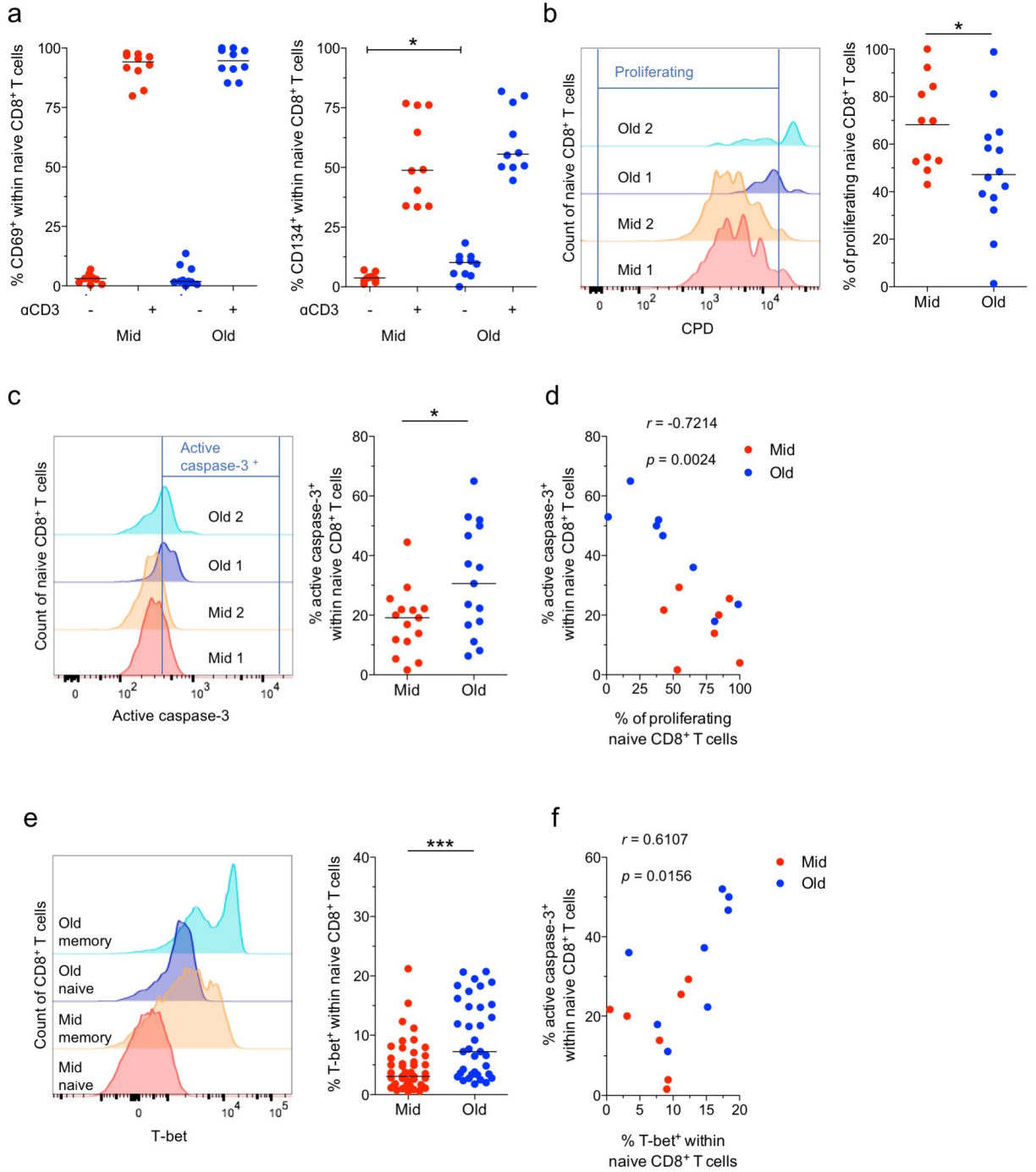
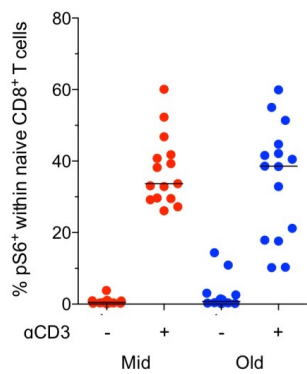


Figure 2

a



b

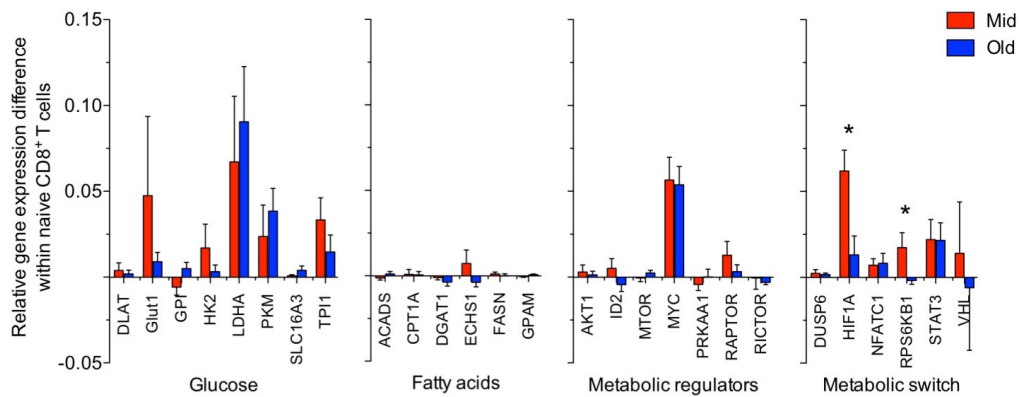
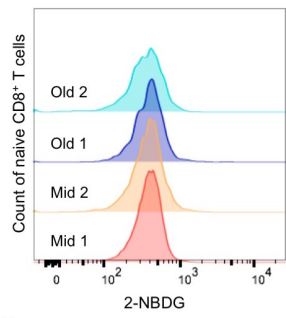
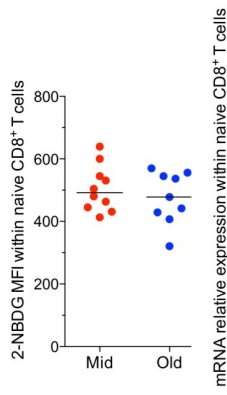


Figure 3

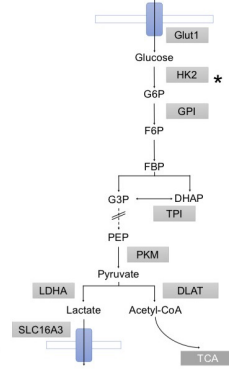
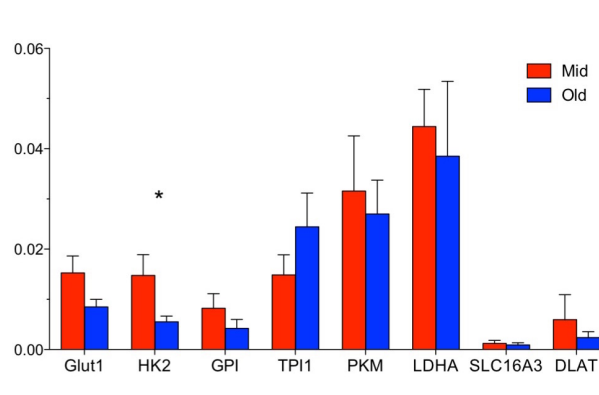
a



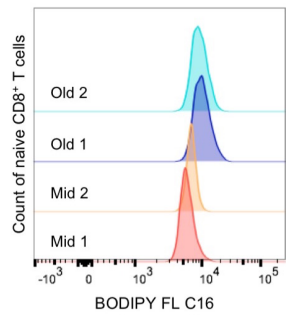
b



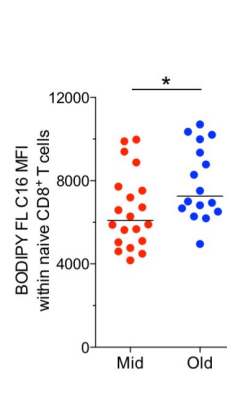
c



d



e



f

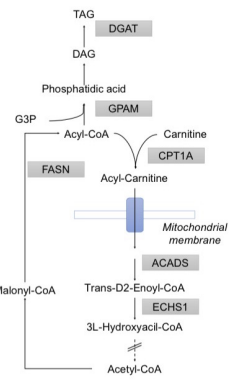
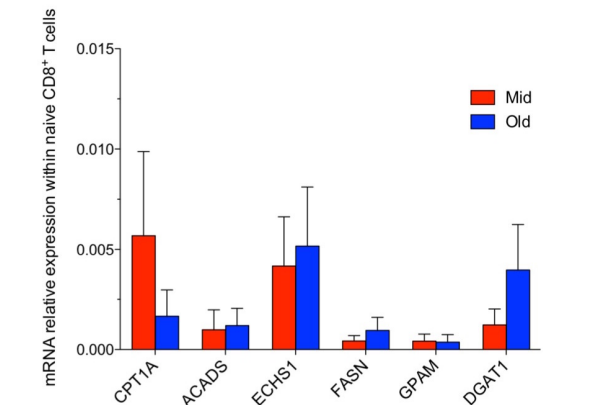
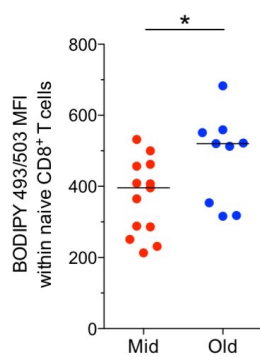
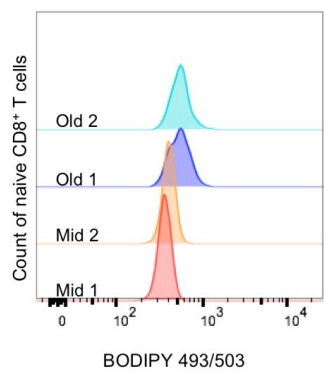
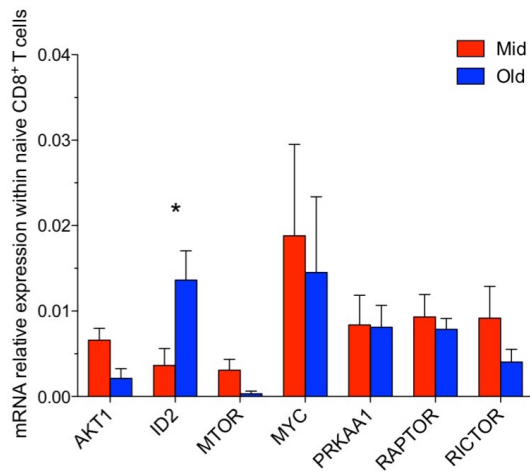


Figure 4

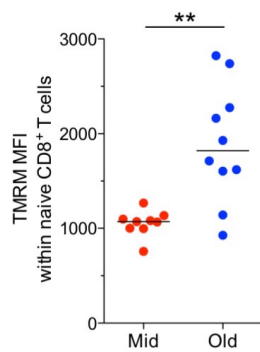
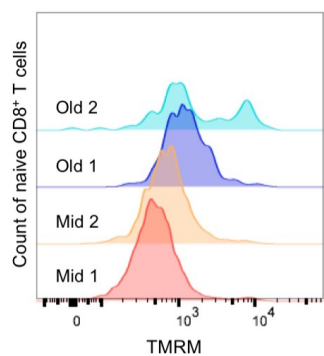
a



b



c



d

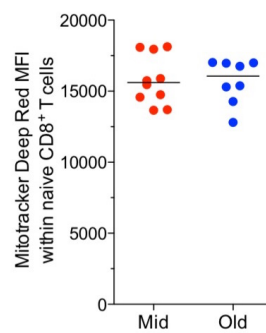
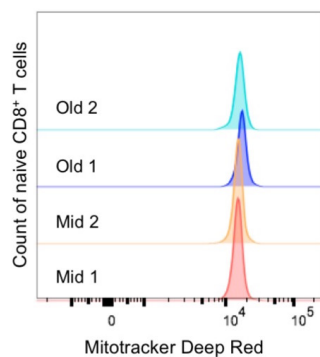


Figure 5

